SYNTHESIS OF N-HEXYL ACETATE BY REACTIVE DISTILLATION

Markus Schmitt*, Hans Hasse*, Klaus Althaus, Hartmut Schoenmakers**,
Lars Götze***, Peter Moritz****

*University of Stuttgart, Institute of Thermodynamics and Thermal Process
Engineering, Stuttgart, Germany
**BASF AG, Process Engineering, Ludwigshafen, Germany
***Sulzer Chemtech Ltd., Winterthur, Switzerland

ABSTRACT

Comprehensive studies on the n-hexyl acetate synthesis by heterogeneously catalyzed reactive distillation are presented. Reactive distillation experiments were carried out both in laboratory and semi-industrial scale with different catalytic packings. Several variants of a basic column set-up and the influence of the most important process parameters were studied. Additionally, phase and chemical equilibria and reaction kinetics were measured. Predictions from stage models of different complexity are compared to the results of experiments. It is shown, that, based on a sound knowledge on reaction kinetics and thermodynamic properties it is possible to successfully describe the studied reactive distillation process.

INTRODUCTION

Reactive distillation combines reaction and separation with the aim to achieve increased conversion, product selectivity or energy savings at favorable investment and operation costs. Theoretical and experimental studies of reactive distillation processes are presently an important focus of both industrial and academic research and development in chemical engineering. For reviews, see e.g. [1, 2].
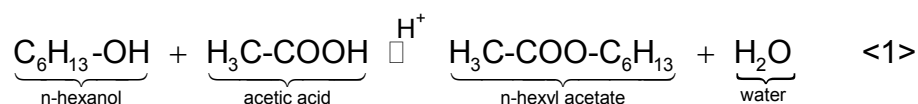
Although reactive distillation has been known for a long time [3] and is being industrially applied in various production lines, e.g. fuel additives, acetates and alkylations [4, 5, 6], many difficulties and challenges still remain. Its high integration density makes reactive distillation a complex process, for which a safe design and direct scale-up to production scale based solely on laboratory experiments and simulations is still far from being state-of-the-art [7]. Models of reactive distillation have to reliably describe phase equilibria and mass transfer as well as chemical equilibria and kinetics and have to take into account the hydrodynamics in structured packings. This remains a considerable challenge [8, 9], especially when the models

are used for different scales and a wide range of operating conditions. As a consequence, the simpler conventional process, in which reaction and distillation are carried out separately, is often favored, even when reactive distillation is principally more attractive. This is one of the reasons, why practical experience with reactive distillation is still limited to comparatively few examples, which is again a considerable obstacle to progress in modeling. The present paper is a contribution to escape from that vicious circle.

The research described in the present paper is carried out under the 5th framework program GROWTH of the European Union as part of the INTINT-project[1] [10]. The focus of that project is on the development of column internals, which can be tailored for specific applications. Five representative test systems have been chosen in the INTINT-project, one of which is the system studied in the present work: the esterification of n-hexanol with acetic acid to n-hexyl acetate and water in a heterogeneously catalyzed reactive distillation column.
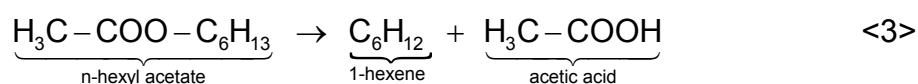
N-HEXYL ACETATE SYSTEM

N-hexyl acetate is a fruity smelling fluid used as flavoring agent or in perfumes. It is produced by the reversible, acid catalyzed liquid phase esterification of n-hexanol and acetic acid, with water as additional product:

$$\underset{\text{n-hexanol}}{C_6H_{13}\text{-OH}} + \underset{\text{acetic acid}}{H_3C\text{-COOH}} \overset{H^+}{\rightleftharpoons} \underset{\text{n-hexyl acetate}}{H_3C\text{-COO-}C_6H_{13}} + \underset{\text{water}}{H_2O} \qquad <1>$$

Since the self-catalyzed reaction is rather slow, reaction <1> is commonly catalyzed using strong inorganic acids, like sulphuric acid, or strongly acidic ion exchange resins. In the present work, the resin *Amberlyst*[®] *CSP2* was used.

In synthesis of n-hexyl acetate, 1-hexene has to be considered as by-product. It can principally either be formed via dehydration of n-hexanol or the pyrolysis of n-hexyl acetate [11].

$$\underset{\text{n-hexanol}}{C_6H_{13}-OH} \overset{H^+}{\rightarrow} \underset{\text{1-hexene}}{C_6H_{12}} + \underset{\text{water}}{H_2O} \qquad\qquad <2>$$

$$\underset{\text{n-hexyl acetate}}{H_3C-COO-C_6H_{13}} \rightarrow \underset{\text{1-hexene}}{C_6H_{12}} + \underset{\text{acetic acid}}{H_3C-COOH} \qquad\qquad <3>$$

Which of these reactions is predominant as side reaction of <1> is not fully under-stood to date.

Table 1 gives an overview over some important thermophysical pure component properties, which are relevant to reactive distillation in the n-hexyl acetate system. Obviously reaction <1> is well suited for reactive distillation as the two reactants are intermediate boilers, whereas the products n-hexyl acetate and water are the heaviest and lightest boiling components, respectively. However, the large boiling temperature difference between the reactants can be unfavorable from the reaction point of view.

Table 1: Characteristic pure component property data [12].

Property	n-hexyl acetate	n-hexanol	acetic acid	water
M / (g/mol)	144.21	102.17	60.05	18.02
T^b(1013 mbar) / °C	171.3	157.2	118.1	100.0
Δh_V(20 °C) / (kJ/kg)	372.9	602.0	386.9	2444.4

The physical properties of the studied system are characterized by strong liquid phase non-idealities, see Table 2. N-hexyl acetate and n-hexanol form a low-boiling homogeneous azeotrope at lower pressures. Heterogeneous azeotropes are observed in the binary systems n-hexyl acetate + water and n-hexanol + water and in the ternary system n-hexyl acetate + n-hexanol + water. Furthermore, dimerization of acetic acid in the gas phase leads to non-ideal behavior, which has to be taken into account.

Table 2: Azeotropic data (calculated with NRTL-parameters from Tables 9 and 10).

Type of azeotrope	Pressure / mbar	Temperature / °C	Mass fraction / (g/g)		
			water	n-hexanol	n-hexyl acetate
Homogeneous, binary	1013	nonexistent			
	300	122.4	---	0.853	0.147
Heterogeneous, binary	1013	97.6	0.578	---	0.422
	1013	97.6	0.667	0.333	---
Heterogeneous, ternary	1013	97.2	0.587	0.184	0.229

REACTIVE DISTILLATION EXPERIMENTS

Experimental Set-ups

Reactive distillation experiments were performed in a 55 mm laboratory column at BASF, Ludwigshafen, Germany, and in a 162 mm pilot-scale column at Sulzer Chemtech, Winterthur, Switzerland. The experimental set-up was similar in both cases and is shown in Figure 1. The column consists of three parts, a reactive section with catalytic packings containing *Amberlyst*® *CSP2*, enclosed by a stripping section below and a rectifying section above. Typically, the rectifying section is not active and overheated by about 20 K. The reflux is then fed on top of the reaction section. N-hexanol (Feed 1) and acetic acid (Feed 2) are fed at the upper and the lower end of the reactive section, respectively, resulting in a counter-current like flow of the reactants in the column.

N-hexyl acetate is separated from n-hexanol in the stripping section and is withdrawn at the bottom (Product). At the column top, phase separation occurs upon condensation because of the heterogeneous azeotropic behavior of the mixture, so that a decanter is used. A small fraction of the organic phase is purged (Dest(org)) to prevent accumulation of the side-product 1-hexene, which is lighter boiling than all substances given in Table 1. The majority of the organic phase is refluxed to the column (RF(org)). In the base case set-up, the aqueous phase is completely withdrawn (Dest(w)). All streams entering the column are preheated to desired temperature. The column top pressure is below ambient, usually in the range from 300 to 500 mbar, to avoid irreversible damage of the catalyst, which can occur above 120 °C.
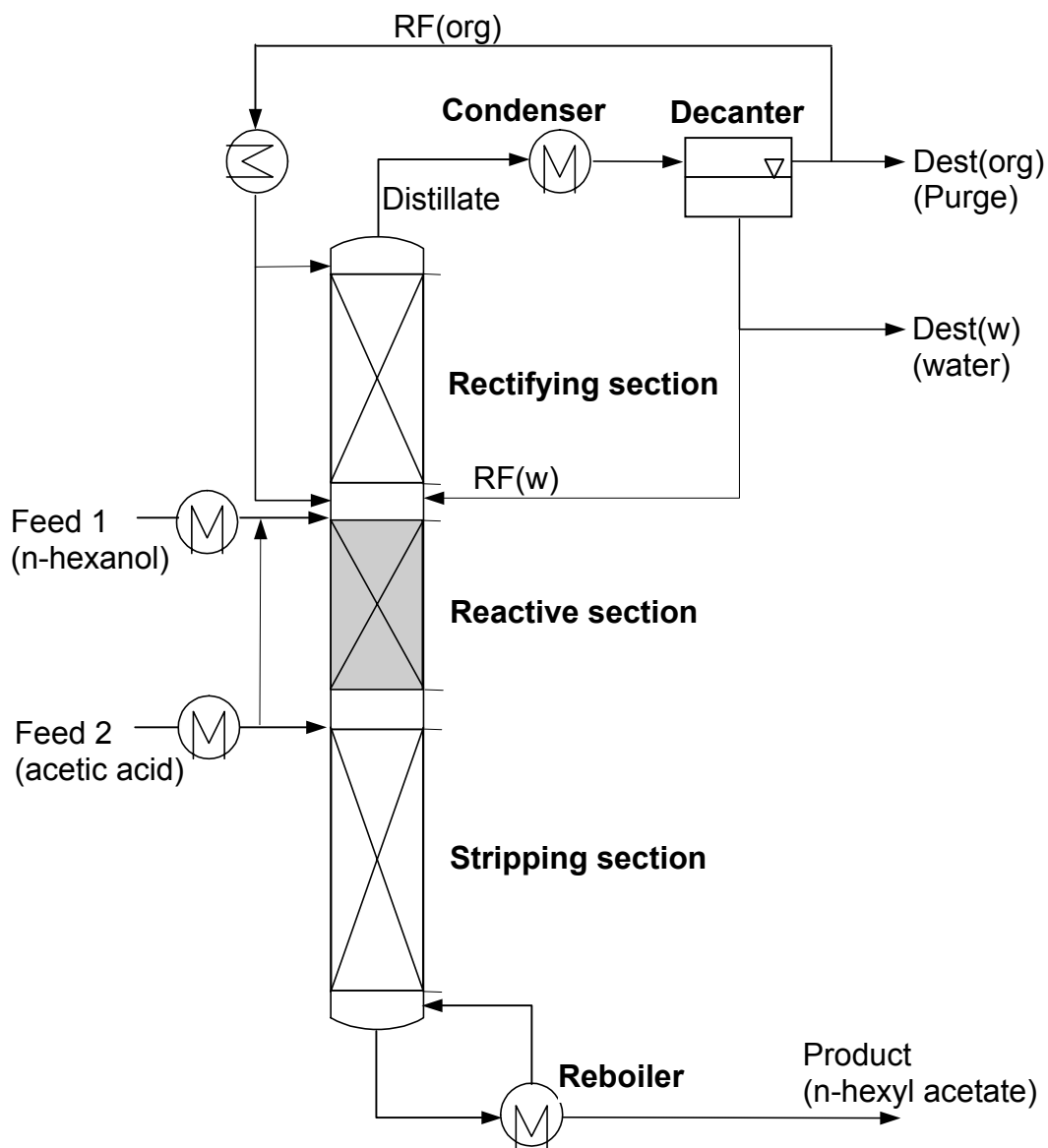

Figure 1: Reactive distillation experimental set-up.

Figure 1 also includes information on studied hardware changes, which are indicated by dashed lines: Operation with active rectifying section (no overheating; reflux on top), partial reflux of the aqueous phase (RF(w)) and variation of the location of Feed 2, which can alternatively be fed together with Feed 1 above the reactive section.

Table 3 gives the most important parameters of the experimental set-ups at BASF and Sulzer Chemtech, underlining the two different scales of operation. It is important to note, that during the laboratory-scale experiments at BASF two different catalytic packings were used, namely *Sulzer Katapak®-S-Laboratory* and *Montz Multipak®-Type II* – for pictures, see Figure 2 –, which have a different structure. *Sulzer Katapak®-S* is a cross-channel structure, where each layer contains catalyst-filled channels, whereas *Montz Multipak®* alternately consists of rectangular catalyst-containing bags and non-reactive mesh-structures used solely for separation. This results in a catalyst amount per reaction section volume, which is almost twice as high for *Montz Multipak®* as for *Sulzer Katapak®-S* as well as a higher separation efficiency of *Montz Multipak®*.

Table 3: Reactive distillation hardware parameters.

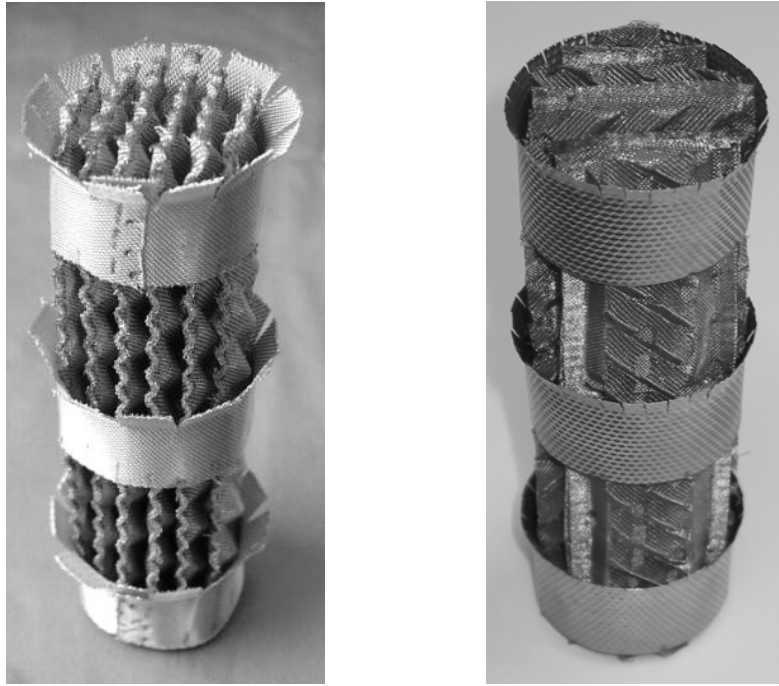| Parameter	Laboratory-scale (BASF)	Pilot-scale (Sulzer Chemtech)
Diameter d / mm	55	162
Adiabatic column operation	Heating jacket	Heating jacket
Rectifying section		
Height h / m	0.5	2.1
Type of Packing	*Sulzer CY*	*Sulzer Mellapak® 500.Y*
NTSM / (1/m)	10	3
Reactive section		
Height h / m	2.0	6.1
Type of Packing	*Sulzer Katapak®-S-Laboratory* or *Montz Multipak®-Type II*	*Sulzer Katapak®-S-250.Y*
NTSM / (1/m)	*Sulzer Katapak®-S-Laboratory*: 3 *Montz Multipak®-Type II*: 4	1
Catalyst type	*Amberlyst® CSP2*	*Amberlyst® CSP2*
Catalyst amount (water swollen) $m_{kat,W}$ / kg	*Sulzer Katapak®-S-Laboratory*: 0.54 *Montz Multipak®-Type II*: 0.96	19.44
Stripping Section		
Height h / m	1.0	3.2
Type of Packing	*Sulzer CY*	*Sulzer Mellapak® 500.Y*
NTSM / (1/m)	10	3

*Figure 2: Pictures of catalytic internals. Left: Sulzer Katapak®-S-Laboratory.
Right: Montz Multipak®-Type II.*

Experimental Procedure

In each experiment, not only the streams entering and leaving the column were monitored (mass flow, composition, temperature) but also composition and temperature profiles were taken, for details see Table 4. In the laboratory-scale experiments at BASF the temperature was measured at nine locations along the column and four liquid composition profile samples were taken in addition to the three samples of the product streams leaving the column. In the pilot-scale experiments at Sulzer Chemtech the temperature profile consisted of nine measurements and, in addition to the samples from the three product streams, five vapor and two liquid phase samples were taken along the column and analyzed.

Sample analysis at BASF was done using gas chromatography in combination with Karl-Fischer-Titration for water content and conventional titration for acetic acid. At Sulzer Chemtech only gas chromatographic analysis was made. The maximum relative error is estimated to be less than 5 % for the gas chromatography and 2 % for the titrations. 100 % tests for the analytical results at BASF show excellent agreement within the given uncertainties.

The mass flow of all input/output streams was measured either directly (mass flow meter or weighing) or indirectly via the volume flow (only for RF(w) and RF(org) in laboratory scale) with an accuracy typically better than 1 % for the direct and 5 % for the indirect measurement. Overall mass balance errors for the whole column are typically below 1 % for the laboratory set-up and 5 % for the pilot plant.

Table 4: Temperature and sample collection locations.

Laboratory scale (BASF)			Pilot scale (Sulzer Chemtech)		
Location from column top	Tem-perature	Samples	Location from column top	Tem-perature	Samples
Top	B_T0	---	Top	S_T0	S_X0 (vapor)
0.5 m	B_T1	---	0.9 m	S_T1	S_X1 (vapor)
1.0 m	B_T2	B_X2 (liquid)	2.1 m	S_T2	S_X2 (liquid)
1.5 m	B_T3	B_X3 (liquid)	4.0 m	S_T3	S_X3 (vapor)
2.0 m	B_T4	---	6.5 m	S_T4	S_X4 (vapor)
2.5 m	B_T5	B_X5 (liquid)	8.2 m	S_T5	S_X5 (liquid)
3.0 m	B_T6	B_X6 (liquid)	9.7 m	S_T6	S_X6 (vapor)
3.5 m	B_T7	---	11.1 m	S_T7	---
Bottom	B_T8	---	Bottom	S_T8	---
Product streams (liquid)	B_Product		Product streams (liquid)	S_Product	
	B_Dest(w)			S_Dest(w)	
	B_Dest(org)			S_Dest(org)	

Experimental Results

Overview

A total of 38 reactive distillation experiments were carried out in the frame of the present work at Sulzer Chemtech and BASF. There were 6 pilot-scale and 32 laboratory-scale experiments, 7 of the latter with *Montz Multipak®-Type II* instead of *Sulzer Katapak®-S-Laboratory*. The experiments can be grouped in 11 different studies with only one parameter being varied at a time. As can be seen from Table 5, virtually all significant process and hardware parameters were studied.

Table 5: Parameter studies.

No.	Process Parameters	No.	Hardware parameters
1	Heat duty	7	Active rectifying section
2	Feed ratio	8	Feed 2 location
3	RF(w) flow	9	Pre-reactor (40 % conversion)
4	Dest(org) flow	10	Scale-up
5	Fluid dynamic load	11	Catalytic internal type
6	Pressure		

To be able to better assess the quality of the experiments, three reproduction runs, in which the same operating point was chosen in independent laboratory-scale experiments, and several stationarity tests were carried out. The reproduction runs confirmed that the relative error of concentrations and flows is typically less than 2 %, the temperatures deviate less than 0.5 K. The runtime of the experiments usually was more than 20 hours, in few cases only five hours. Stationarity tests showed, that even after three hours key concentrations were as close as 5 % (relative) to their final value. Another important quality criterion is that the internal liquid load, which ranged from 5 to 9 $m^3/(m^2h)$, was within typical operation range of the catalytic packings used.

Parameter study results

From the plentiful data collected in these studies, only a few covering especially interesting effects are selected for presentation in the frame of the present paper. The idea is to give an insight into the behavior of reactive distillation in the studied system, to examine the effect of the two different catalytic packings and to address the scale-up problem.

Heat duty study

Five experiments were carried out in the laboratory scale with *Sulzer Katapak®-S-Laboratory* to study the influence of heat duty on the reactive distillation process. The results are presented in Figure 3, where the conversion of acetic acid and the product purity, i.e. the n-hexyl acetate mass fraction in the Product-stream, are shown as a function of the total mass flow leaving the top of the column (Distillate). The heat duty itself is not chosen as independent variable because of unknown heat losses, whereas the Distillate flow was measured directly. The heat duty was varied from 1030 W to 1500 W corresponding to Distillate flows from 2270 to 5200 g/h. Figure 3 shows that the conversion as well as the product purity decrease with increasing heat duty (increasing Distillate flow). The reason for this behavior is that with the increasing heat duty the reflux increases (Dest(w)- and Dest(org)-flows are constant), which leads to a disadvantageous separation of the reactants, resulting in a reduced acetic acid concentration in the liquid phase in the reaction zone. In the range of heat duties studied here, this effect obviously outweighs the benefits from the enhanced removal of the products from the reactive section.
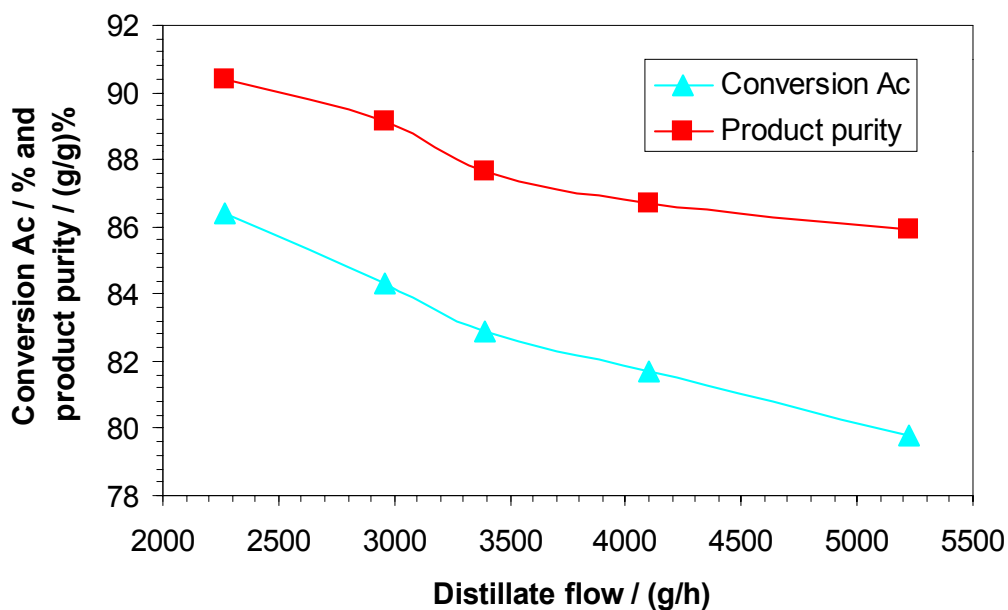

Figure 3: Heat duty study (experimental results).

Aqueous reflux study

Usually, only the organic phase from the decanter is recycled to the column, whereas the aqueous phase is completely withdrawn. A process variant, in which a part of the aqueous phase is used as additional reflux, is of major interest, especially regarding its potential to control temperature in the reaction zone. Five laboratory-scale experiments with the catalytic internal *Sulzer Katapak®-S-Laboratory* were made to study the effects of that option. The amount of the aqueous reflux (RF(w)-stream) was varied from 0 to 1380 g/h, corresponding to a mass-based ratio between RF(w) and Dest(w) ranging from 0 to about 3.

Results from the aqueous reflux study are summarized in Figure 4, which shows three different regions. In Region I, up to aqueous reflux flows of about 1000 g/h, conversion and product purity monotonously increase. This can be understood considering that the water refluxed to the column is lightest boiler and has a specific enthalpy of vaporization 5 to 7 times higher than that of the other components (see Table 1). Thus, to evaporate refluxed water within one or two theoretical stages below the RF(w)-feed, organic compounds in the vapor have to condense, leading to higher concentrations of reactants in the liquid phase in the reactive section and, consequently, a higher conversion. However in Region II – at aqueous reflux flows above about 1000 g/h – this advantageous effect is outweighed by the high water concentrations in the upper part of the reaction zone, reducing the rate of n-hexyl acetate formation and leading to a decline of temperature in this section (temperatures B_T2 and even B_T3), which again affects the reaction rate. At still higher aqueous reflux flows above about 1300 g/h (Region III), reasonable column operation is not possible anymore, as the amount of organic compounds in the vapor is too small to evaporate the refluxed water. This leads to high water concentrations all over the column, extremely low temperatures, and hence, insufficient conversion. Since in the experiment in that operation point even after nine hours no stabile operation was achieved, no data details can be given for Region III in Figure 4.

It should be noted, that the decline of temperature (and conversion) in Region II is very sensitive to the water reflux and large changes of the column's operating point follow even small changes of the amount of aqueous reflux. Due to these problems, the option to control the temperature in the reaction zone by means of the aqueous reflux on top of the reaction zone is not recommended.
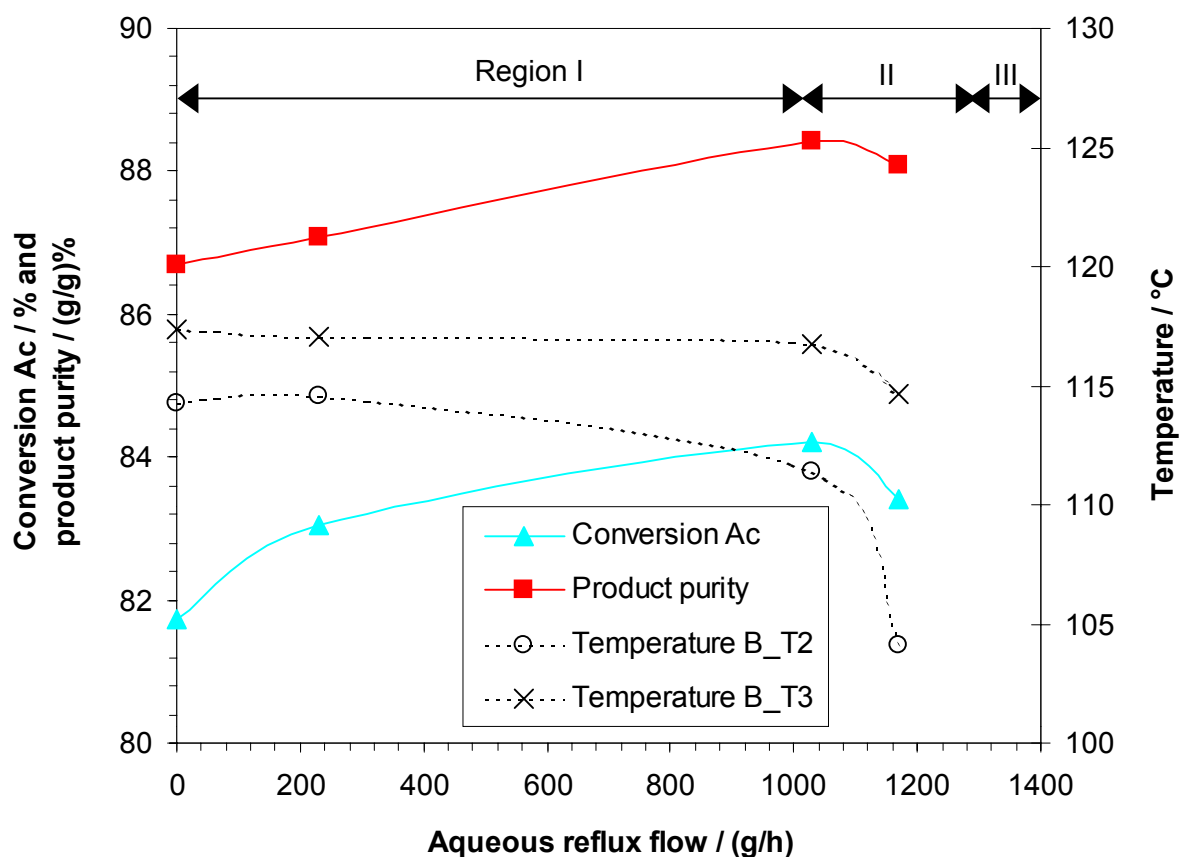
Figure 4: Aqueous reflux study (experimental results).

Catalytic packing study

Seven of the laboratory-scale experiments were made using *Montz Multipak[®]-Type II* instead of *Sulzer Katapak[®]-S-Laboratory*, while all operating conditions were kept the same. An example for results from that comparison of the two different internals, a feed ratio study (ratio of n-hexanol with respect to acetic acid in the total feed), is given in Figure 5. As expected, both internals show an increase of acetic acid conversion with increased excess of n-hexanol and a decrease of product purity due to the excess n-hexanol, which leaves the column via the Product stream. *Montz Multipak[®]-Type II* gives a favorably higher conversion and product purity than *Sulzer Katapak[®]-S-Laboratory*, which simply is a consequence of the fact that the amount of catalyst per volume in both packings differs by about a factor of 2 (compare Table 3).

It is worthwhile to mention, that some of the parameter studies carried out with *Montz Multipak[®]-Type II* show a significant scattering of the data, which was not observed with *Sulzer Katapak[®]-S-Laboratory*. The reason for this effect might be that the requirements regarding liquid distribution are especially high for *Montz Multipak[®]-Type II* and were perhaps not fully met with the single centrical liquid dripping position used in the laboratory experiments. Liquid distribution strongly affects the interaction between the catalytic bags and the non-catalytic separation layers in *Montz Multipak[®]-Type II* and is not easy to control in small-scale experiments.
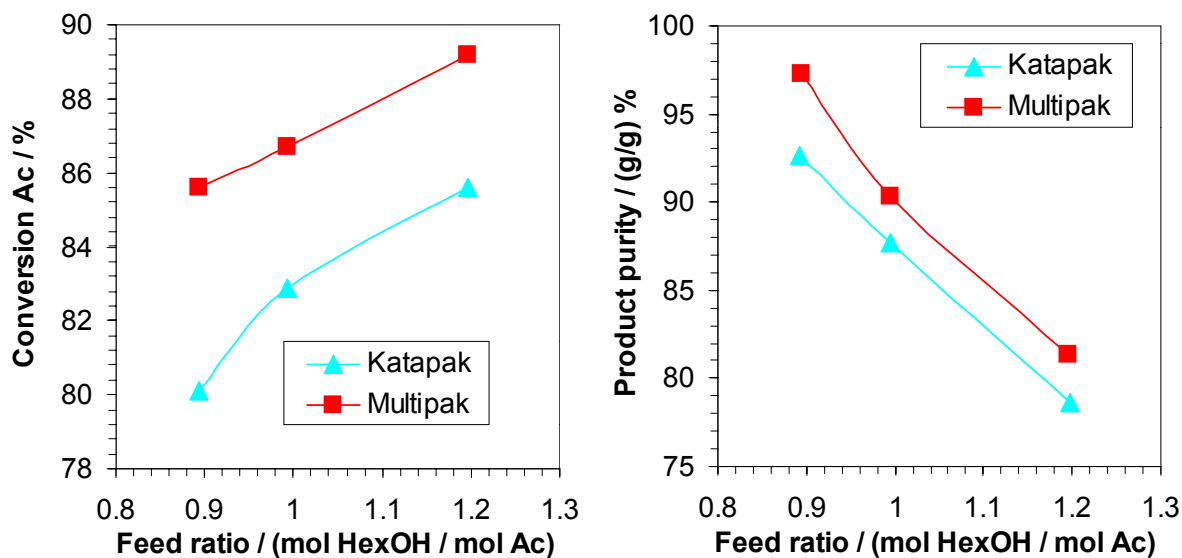
Figure 5: Comparison between internals Montz Multipak[®]-Type II and Sulzer Katapak[®]-S-Laboratory for the feed ratio study (experimental results).

Scale-up study

With the laboratory-scale experiment B_V28 and pilot-scale experiment S_V05, the attempt was made to perform a direct scale-up, i.e., to have identical hydrodynamic load and separation capacity, the scale-up ratio by cross-sectional area being 1 : 8.6. In Table 6 all relevant parameters are compared for both experiments. The column set-up is identical for both experiments, complying with the base-case set-up described above but with an active rectifying section. All process parameters not mentioned in Table 6 were the same (column top pressure, feed ratio, pre-heater temperatures…). Considering all parameters, an almost perfect scale-up was achieved, the only (unavoidable) difference important to mention being the almost four times higher amount of catalyst per amount of feed in the pilot-scale column.

Table 7 summarizes some key results from the two experiments in different scales. Conversion of n-hexanol is significantly higher in the pilot-scale compared to the laboratory-scale, resulting in virtually pure n-hexyl acetate as bottom product. Since the temperature in the reactive section is identical in both scales, this increase in conversion is due to the much higher catalyst amount in the pilot plant.

However, the high reaction capacity also leads to disadvantages. Probably because of the large reactive section (6 m length) at high temperature (130 °C) and high n-hexyl acetate concentration (up to 0.8 g/g), the 1-hexene side-product formation enormously increased (cf. reaction equation <3>), reducing the selectivity of n-hexanol to n-hexyl acetate by more than 10 %. That result clearly points out the importance of migitation of side reactions in reactive distillation design, a problem, which is addressed in presently ongoing studies.

Table 6: Scale-up: comparison of parameters.

	B_V28 (laboratory scale)	S_V05 (pilot scale)
Internals		
Reactive section	*Sulzer Katapak®-S-Laboratory*; NTS = 6; Catalyst *Amberlyst® CSP2*	*Sulzer Katapak®-S-250.Y* NTS = 6; Catalyst *Amberlyst® CSP2*
Rectifying and stripping section	*Sulzer CY*; NTS = 15	*Sulzer Mellapak® 500.Y*; NTS = 16
Scale-up parameters		
Total feed per cross-section area / (kg/m^{2}h)	1536.4	1673.8
Total condensate per cross-section area / (kg/m^{2}h)	1809.9	2081.4
Dest(org) per cross-section area / (kg/m^{2}h)	193.6	203.8
Catalyst amount per feed / (kg$_{Kat}$ /kg$_{Feed}$ /h)	0.147	0.563

Table 7: Results of scale-up experiments B_V28 and S_V05.

Parameter compared	B_V28 (laboratory-scale)	S_V05 (pilot-scale)
Conversion n-hexanol / %	83.9	93.8
Product purity / (g/g)%	91.1	99.5
Selectivity HexOH to HexAc / %	96.2	85.9
Selectivity HexOH to HEN / %	0.1	6.3
Mean temperature in reactive section / °C	129.7	130.2

MODELLING AND SIMULATION

Two different types of reactive distillation models were developed, parameterized and compared in simulations in the present work. Both models are based on the stage concept and use the assumption of vapor-liquid equilibrium on each stage. In *Model #1* it is furthermore assumed that chemical equilibrium is reached on each stage, whereas in *Model #2* chemical reaction kinetics in the liquid bulk phase are considered. In both models liquid phase non-idealities are taken into account by the NRTL-model and the gas phase is assumed to be ideal, except for the acetic acid dimerization, which is modeled by chemical theory.

Data Sources
The models mentioned above require the following input:
- *Pure component thermophysical data:* vapor pressure, heat capacity and enthalpy of vaporization, dimerization equilibrium constant (only acetic acid),
- *Binary thermophysical data:* NRTL-model parameters,
- *Reaction data:* chemical equilibrium constants and reaction kinetics.

Most of the thermophyiscal data can be found in databases, but for some binary systems, information was missing. Furthermore, no reaction data were available in open literature. These gaps were filled in the present project.

Phase equilibrium data
The n-hexyl acetate system with its four main components according to reaction equation <1> consists of six binary subsystems. Table 8 shows for which of these subsystems phase equilibrium data were available in the literature [13].

Table 8: Binary phase equilibrium data available from literature.

	n-hexanol	n-hexyl acetate	water
acetic acid	VLE	**NO DATA**	VLE
n-hexanol	---	**NO DATA**	VLE + LLE
n-hexyl acetate	---	---	VLE + LLE

The NRTL-model has been chosen for the description of the phase equilibrium data. The model equations can be found in [14] and the parameters G_{ij} and τ_{ij} are defined as follows:

$$G_{ij} = \exp\left(-\alpha_{ij} \cdot \tau_{ij}\right) \tag{1}$$

$$\tau_{ij} = \frac{\left(g_{ij} - g_{jj}\right)}{\mathbf{R} \cdot T} = a_{ij} + \frac{b_{ij}}{T/\mathrm{K}} \tag{2}$$

The NRTL-parameters a_{ij}, b_{ij} and α_{ij} of the four systems for which data were available in literature are given in Table 9.

Table 9: NRTL-parameters for water + n-hexyl acetate, water + n-hexanol, water + acetic acid and acetic acid + n-hexanol.

Component i	water	water	water	acetic acid
Component j	n-hexyl acetate	n-hexanol	acetic acid	n-hexanol
a_{ij}	-1.7481	18.5100	1.8053	0.0
a_{ji}	-1.3148	3.4660	-0.7455	0.0
b_{ij}	3545.58	-3501.50	-86.26	-269.12
b_{ji}	998.70	-690.50	119.06	579.91
$\alpha_{ij} = \alpha_{ji}$	0.2	0.3	0.3	0.3

For the two binary systems acetic acid + n-hexyl acetate and n-hexanol + n-hexyl acetate, for which data were missing, vapor-liquid equilibrium experiments were carried out. This has been done using a recirculation still similar to that described in [15]. About 80 data points were taken at pressures of 300, 600 and 900 mbar. NRTL-parameters were fitted to all these data. The results are given in Table 10. As an example, Figure 6 presents the isobaric *McCabe-Thiele* diagrams at 300 mbar for

both binary systems, including experimental data points and their correlation with the NRTL-model.

Table 10: NRTL-parameters for acetic acid + n-hexyl acetate and n-hexanol + n-hexyl acetate from experimental data measured in the present work.

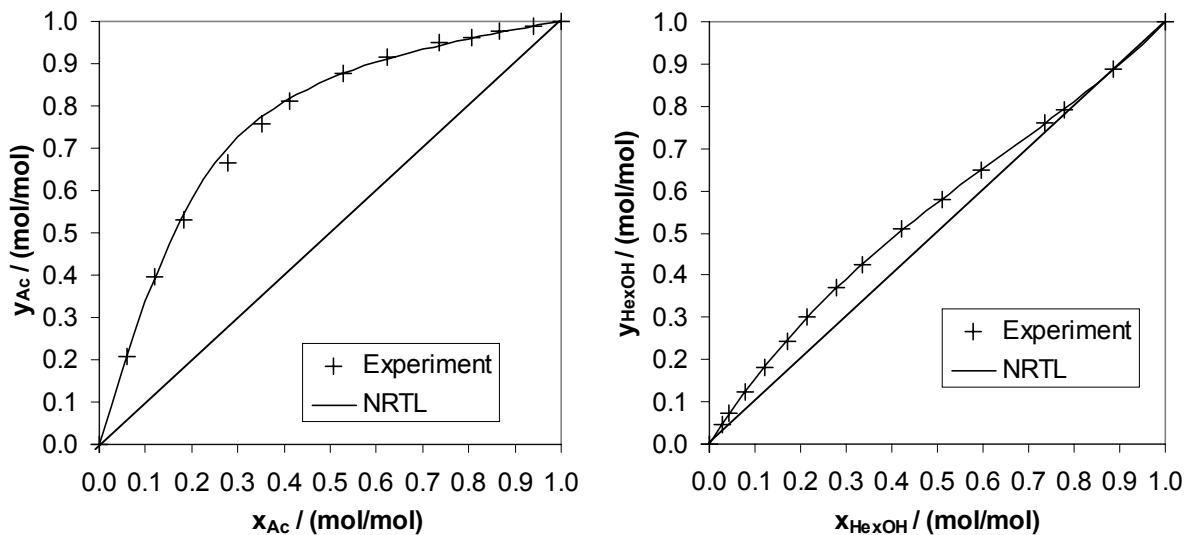| Component i	acetic acid	n-hexanol
Component j	n-hexyl acetate	n-hexyl acetate
a_{ij}	4.2895	3.2413
a_{ji}	- 5.4563	- 4.0646
b_{ij}	-1489.92	- 1049.70
b_{ji}	2184.61	1522.47
$\alpha_{ij} = \alpha_{ji}$	0.3	0.3

Figure 6: McCabe-Thiele diagrams for acetic acid + n-hexyl acetate and n-hexanol + n-hexyl acetate at 300 mbar.

These results complement the database on the vapor-liquid equilibria in the binary subsystems of the quaternary system under investigation. The correlation of the binary vapor-liquid equilibrium data with the NRTL-model gives good results in all cases. However, using model parameters determined from vapor-liquid equilibrium experiments to predict multicomponent experimental data on liquid-liquid equilibria, results only in insufficient agreement. Work on multicomponent liquid-liquid equilibrium data is still in progress. Additionally, multicomponent vapor-liquid equilibrium data is presently measured as well, in order to test the predictions from the binary data.

Reaction data
Modeling reactive distillation requires information on chemical equilibrium and in most cases on reaction kinetics.

For the reaction kinetic measurements, a laboratory plug flow reactor (d = 10 mm; L = 568 mm; 5 sample valves along the reactor) filled with *Amberlyst*® *CSP2* was used, because it allows operation at conditions similar to those present in a reactive distillation column with catalyst-filled internals. Steady-state operation is important for the reaction kinetic experiments because the swelling state of the catalyst resin and thus its catalytic properties depend on the surrounding bulk concentration. Hydrodynamic similarity to the conditions in the catalyst-filled channels of structured packings like *Sulzer Katapak*®*-S* was not fully achieved, due to limitations in the capacity of the feed pump of the laboratory reactor.

Reaction kinetic experiments were planned on the basis of preliminary reactive distillation simulations to determine the relevant temperature and concentration range. A total of 26 reaction kinetic experiments were carried out with liquid loads in the range from 2.3 to 3.5 $m^3/(m^2_{Kat,W}\ h)$ (reference: bulk cross-sectional area of catalyst in water-swollen form). Four reproduction runs show relative deviations of typically less than 3 %. An influence of mass transport was observed, but not accounted for in the kinetic model presented here.

Detailed modeling of the heterogeneously catalyzed reaction kinetics should take the physical properties of the ion exchange resin into account, i.e. the considerably different concentrations in the resin compared to the bulk. This can be done using an adsorption approach [16] [17] or by describing the behavior of the polymer phase, e.g. with an extended Flory-Huggins-model [18]. However, both model types require separate information from swelling experiments, which was not available for the present study. Therefore, the reaction kinetic data were modeled using a simple pseudo-homogeneous approach for the reaction rate. A second order rate equation formulated in activities was used:

$$\frac{\mathrm{d}n_j}{\mathrm{d}t} = c_{cat,H^+} \cdot V^S_{cat,W} \cdot \left(\nu_{1,j} \cdot k^a_1\left(T\right) \cdot a_{HexOH} \cdot a_{Ac} + \nu_{-1,j} \cdot k^a_{-1}\left(T\right) \cdot a_{HexAc} \cdot a_W \right) \quad (3)$$

where

$$a_j = x_j \cdot \gamma_j \quad \text{with } j = 1..N. \quad (4)$$

The temperature dependence of the rate constants k^a_1, k^a_{-1} was modeled using the *Arrhenius* approach

$$k^a_i\left(T\right) = k^a_i\left(T^0\right) \cdot \exp\left[-\frac{E_i}{\mathbf{R}} \cdot \left(\frac{1}{T} - \frac{1}{T^0} \right) \right] \quad \text{with } i = 1, -1. \quad (5)$$

As can be seen from Equation (3), the reaction rate is related to the bulk volume of catalyst resin in water-swollen form. This is reasonable because catalytic packings typically are delivered filled with catalyst in this swelling state and this parameter is easy to determine. The simple reaction kinetic model described above does not take mass transport limitations into account, so that its applicability is limited to hydrodynamic conditions similar to those present in the reaction kinetic experiments.

The four parameters of the reaction kinetic model were fitted to all experimental reaction kinetic data. The results are given in Table 11. Figure 7 shows a typical comparison between simulation and experimental data, which agree reasonably. It is worthwhile to mention, that the molar energies of activation of forward and back reaction are the same, which means the heat of reaction is virtually zero.

Table 11: Reaction kinetic model parameters.

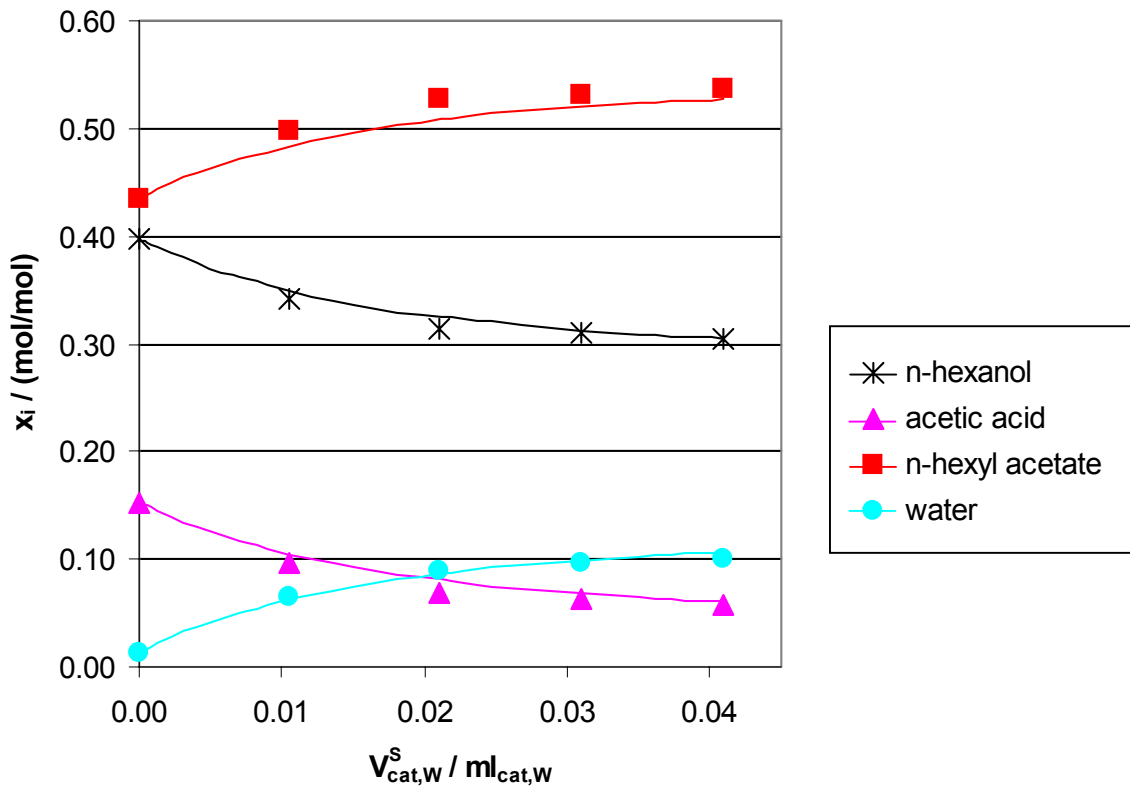| Fitted parameters			
$k_1^a(T^0)/(\mathrm{mol/s \cdot mol_{H^+}})$	$k_{-1}^a(T^0)/(\mathrm{mol/s \cdot mol_{H^+}})$	$E_1/(\mathrm{J/mol})$	$E_{-1}/(\mathrm{J/mol})$
0.02219	0.000695	34350	34350
Additional data			
T^0/K	$c_{cat,H^+}/(\mathrm{mol_{H^+}/l_{cat,W}})$		
373.15	1.7		

Figure 7: Reaction kinetics: experimental data (symbols) from a plug flow reactor and model correlation (solid lines).

Chemical equilibrium information can be obtained from the reaction kinetic model described in Equation (3) for the limit of zero reaction rate. Then Equation (3) yields:

$$\frac{k_1^a}{k_{-1}^a} = \prod_{j=1}^{N}(a_j)^{\nu_{1,j}} \qquad (6)$$

A comparison of Equation (6) with the expression for the chemical equilibrium constant that can be derived from standard thermodynamics neglecting the pressure dependence of the chemical potential:

$$K_1(T) = \prod_{j=1}^{N} (a_j)^{v_{1,j}} ,$$ (7)

results in

$$K_1(T) = \frac{k_1^a}{k_{-1}^a} .$$ (8)

Equation (8) together with Equation (5) allows the calculation of the chemical equilibrium constant $K_1(T)$ from the parameters given in Table 10. Furthermore Equations (6) to (8) show the consistent modeling of reaction rate and chemical equilibrium.

To complement the chemical equilibrium constant obtained through Equation (8) from the reaction kinetic experiments, batch-cell equilibrium experiments were carried out in the temperature range of interest, i.e. at 80, 90, 100, 110 and 120 °C. A total of about 100 data points were taken. These data show very good agreement with the model described above. The individual numbers for chemical equilibrium constant scatter around the correlation within the experimental uncertainty, thus confirming the reliability of the reaction kinetic measurements in the plug flow reactor.

Simulation of Reactive Distillation Experiments
Based on the correlations described above, the Models #1 (phase equilibrium + chemical equilibrium) and #2 (phase equilibrium + bulk reaction kinetics) allow the simulation of the reactive distillation experiments. These simulations are predictions in the sense, that no information on the reactive distillation experiment is used. The simulations with Model #2 result in an under-prediction of the observed conversion. This is caused by the fact that the liquid loads used in the laboratory reactor were significantly lower than those in reactive distillation experiments. Hence, mass transport limitations, which lead to apparently slower kinetics in the laboratory reactor, are less important in the reactive distillation experiments.

In a first attempt, a very simple procedure was used to overcome that problem. An acceleration factor was introduced in the reaction rate equation (3). First, individual acceleration factors for each laboratory-scale experiment with *Sulzer Katapak®-S-Laboratory* were determined by a fit to the measured acetic acid conversion. From these numbers, a mean acceleration factor was calculated, yielding as result 1.38, i.e. the apparent reaction rate in the reactive distillation column is 38 % larger than that expected from the plug-flow-reactor experiments. Deviations of the individual acceleration factors from the mean acceleration factor are typically only about 5 %. Because of these small deviations and the reasonable order of magnitude the mean acceleration factor was adopted for all simulations in the frame of the present study.

Work is on the way to perform reaction kinetic measurements in the liquid load range present in reactive distillation columns and to explicitly include the mass transport

limitations in the model. It will then be possible to avoid the use of the empirical acceleration factor, and, hence, come to a fully predictive model.

It should also be mentioned that the 1-hexene-formation observed in the pilot-plant experiments was not explicitly included in the model as reaction kinetic information on that side reaction is not available at present. Therefore, it was taken into account by using a virtual 1-hexene feed. In accordance with reaction equation <2>, the n-hexanol feed was reduced by the mole flow of 1-hexene and additional water was fed in equimolar amount of the 1-hexene flow. Following this procedure the column material balance is still satisfied. The binary interaction parameters of 1-hexene with all other components were estimated using modified UNIFAC method [19]. Due to the high relative volatility of 1-hexene compared to the other components, the results of the simulation of the reactive distillation column are not sensitive regarding the assumptions described above.

As mentioned in the section *Phase equilibrium data*, multicomponent liquid-liquid equilibrium could not be modeled with required quality at the present stage of the project. Therefore the decanter was not explicitly simulated, but the reflux to the column was set according to the experimental data.

For the comparison of the results of the reactive distillation experiments with the model predictions, only a few, typical examples are discussed here. The results for the experiments B_V06 and S_V05, which are base cases for the studies in the laboratory scale and the pilot scale, respectively, were chosen. These results are typical for the experiments with *Sulzer Katapak*®-*S*. In modeling the experiments with *Montz Multipak*® ambiguous results were obtained. Some experiments are described in a quality similar to that obtained for *Sulzer Katapak*®-*S*, in other cases large deviations occur. This is interpreted as an effect of the difficulties with the liquid distributor already discussed above.

Figure 8 shows the results of the pilot-scale experiment S_V05 and Figure 9 contains similar information for the laboratory-scale experiment B_V06. The predictions with Model #1 are poor and sometimes even fail to give qualitative trends. Contrarily, Model #2, which takes reaction kinetics explicitly into account, shows excellent qualitative and good quantitative agreement with the experimental data for both scales. This is in agreement with the observations made by Moritz et. al. [20] for the heterogeneously catalyzed reactive distillation of methyl acetate, when comparing simulation results obtained with various types of models with experimental data. It has to be emphasized, that the results of the pilot-plant experiments have not been included in the determination of the mean acceleration factor, i.e. for those experiments the simulation is entirely predictive.
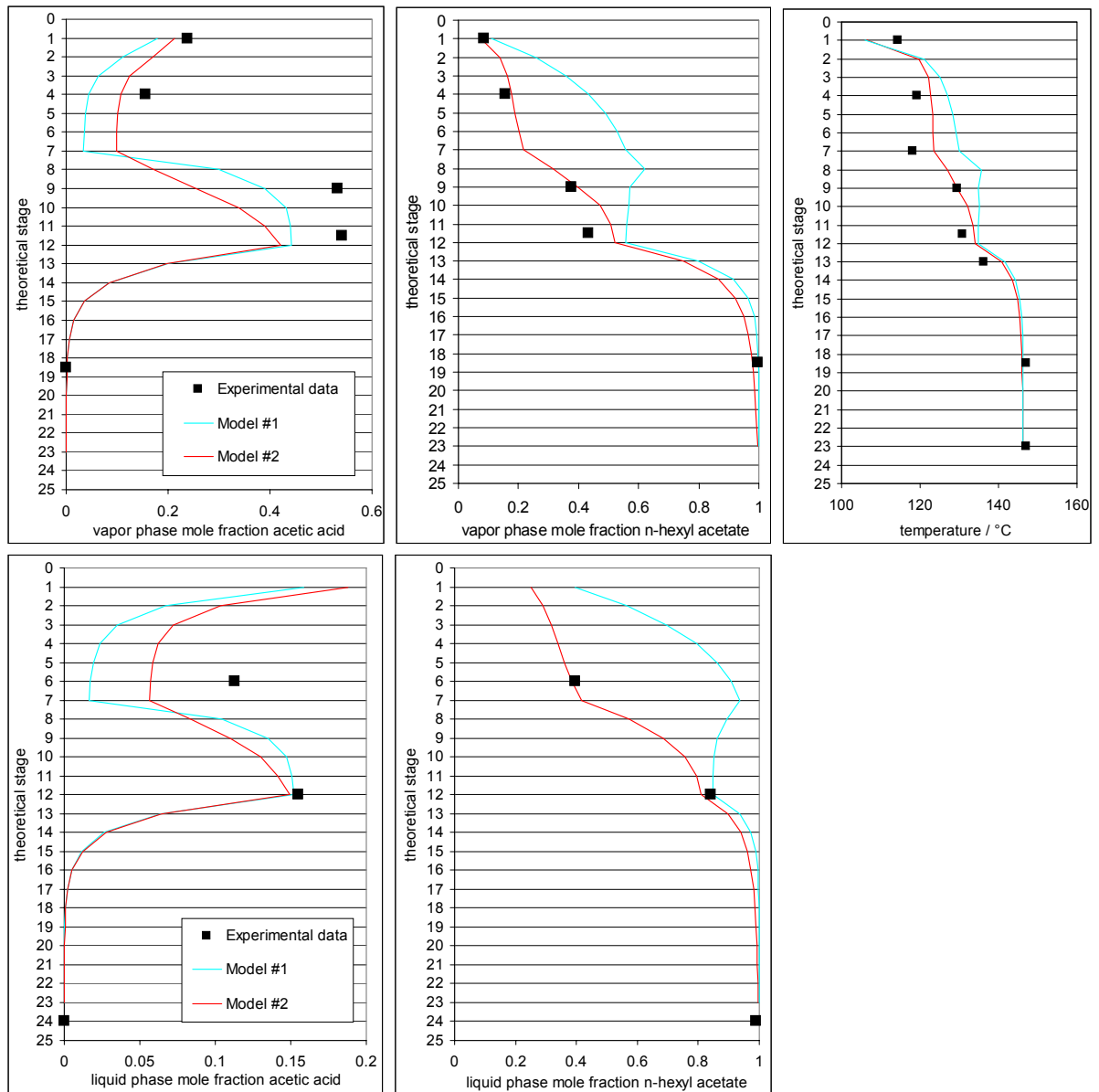
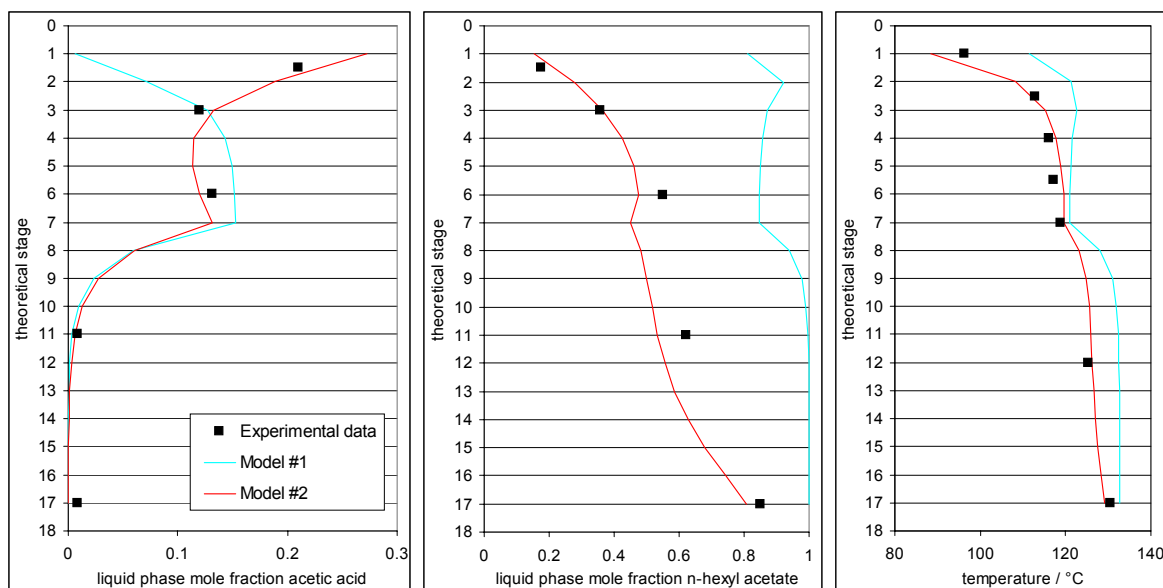*Figure 8: Experiment S_V05 (pilot scale; Sulzer Katapak®-S-250.Y).*

Figure 9: Experiment B_V06 (laboratory scale; Sulzer Katapak®-S-Laboratory).

CONCLUSIONS

The n-hexyl acetate esterification is introduced as a new test system for heterogeneously catalyzed reactive distillation. The experimental studies carried out for that system in the frame of the present work range from the determination of phase and chemical equilibrium and reaction kinetic data to reactive distillation experiments in laboratory scale (column diameter 55 mm, packing height 3.5 m) and pilot-plant scale (column diameter 162 mm, packing height 11.3 m) with two different types of internals (*Sulzer Katapak®-S* and *Montz Multipak®*). This database is one of the broadest available in the open literature for reactive distillation systems.

Correlations for thermophysical and reaction data are presented and used in two different stage-based models for process simulation. Model #1, based on the assumption of both phase and chemical equilibrium on each stage, is not able to correctly predict the reactive distillation experiments, whereas Model #2, which takes reaction kinetics in the liquid phase into account, gives good qualitative and quantitative agreement with the reactive distillation experiments both for the laboratory and the pilot scale.

Work on the n-hexyl acetate reactive distillation system is still in progress. Future developments will comprise an improved version of the reaction kinetic model, taking adsorption as well as mass transfer explicitly into account and improvements in the simulation of the liquid-liquid phase split in the decanter. Furthermore, a rate-based model will be tested on the experimental data in cooperation with University of Dortmund, where such a model has been developed [21]. Additionally, one more reactive distillation experimental series in the pilot-plant scale will be carried out with a newly developed modified internal.

NOMENCLATURE

Latin Symbols

a	activity
a	NRTL-parameter
b	NRTL-parameter
c_{cat,H^+}	total capacity of ion exchange resin (catalyst)
d	diameter
E	molar activation energy
g	molar *Gibbs* free enthalpy
G	NRTL-parameter
h	height
Δh_v	specific enthalpy of vaporization
K	thermodynamic chemical equilibrium constant
L	length
k^a	activity-based reaction rate constant
M	molecular weight
n	mole number
N	total number of components
$\mathbf{R}$	ideal gas constant (8.314 J/(mol K))
t	time
T	temperature
V	volume
x	liquid phase mole fraction
y	vapor phase mole fraction

Greek Symbols

α	NRTL-parameter
γ	activity coefficient normalized according to *Raoult*
τ	NRTL-parameter
ν	stoichiometric coefficient

Index

0	reference
1, -1	forth and back reaction
b	boiling
i	index for reactions and for components
j	index for components
S	bulk

Abbreviations

Ac	acetic acid
cat	catalyst
HEN	1-hexene
HexAc	n-hexyl acetate

HexOH	n-hexanol
NTS	number of theoretical stages
NTSM	number of theoretical stages per meter of packing
W	water / water-swollen

REFERENCES

1. M. F. Doherty and G. Buzad (1992): Reactive distillation by design. Trans IChemE, 70, Part A, 448-458.

2. R. Taylor and R. Krishna (2000): Modelling reactive distillation. Chem. Eng. Sci., 55, 5183-5229.

3. A. A. Backhaus (1921): Continuous processes for the manufacture of esters, US patent no. 1400849.

4. J. L. DeGarmo, V. N. Parulekar and V. Pinjala (1992): Consider reactive distillation. Chem. Eng. Prog., 88 (3), 43-50.

5. V. H. Agreda, L. R. Partin and W. H. Heise (1990): High-purity methyl acetate via reactive distillation. Chem. Eng. Progr., 86 (2), 40-46.

6. J. D. Shoemaker and E. M. Jones (1987): Cumene by catalytic distillation. Hydrocarbon Processing, 57-58.

7. M. F. Malone and M. F. Doherty (2000): Reactive distillation. Ind. Eng. Chem. Res., Commentaries, 39, 3953-3957.

8. H. Hasse (2000): Thermodynamics of reactive separations. In: K. Sundmacher, A. Kienle: Reactive Distillation, Wiley-VCH, Weinheim (in press).

9. P. Moritz and H. Hasse (1999): Fluid dynamics in reactive distillation packing Katapak-S. Chem. Eng. Sci., 54, 1367-1374.

10. European Union project (2000): Intelligent column internals for reactive separations (INTINT). Competitive and sustainable growth (GROWTH) programme, GRD1-CT1999-10596.

11. K. Peter and C. Vollhardt (1987): Organic chemistry. W. H. Freeman and company, New York and Oxford.

12. R. H. Perry and D. W. Green (1997): Perry's Chemical Engineers' Handbook. 7th edition, McGraw-Hill, New York.

13. J. Gmehling and U. Onken (1991): DECHEMA Chemistry Data Series. 2nd edition, Schön & Wetzel, Frankfurt/Main.

14. H. Renon and J. M. Prausnitz (1968): Local compositions in thermodynamic excess functions for liquid mixtures. AIChE Journal, 14, 135-144.

15. L. Rafflenbeul and H. Hartmann (1978): Eine dynamische Apparatur zur Bestimmung von Dampf-Flüssigkeits-Phasengleichgewichten. Chemie Technik, 4, 145-148.

16. T. Pöpken, L. Götze and J. Gmehling (2000): Reaktion kinetics and chemical equilibrium of homogeneously and heterogeneously catalyzed Acetic Acid esterification with Methanol and Methyl Acetate hydrolysis. Ind. Eng. Chem. Res., 39, 2601 – 2611.

17. A. Rehfinger and U. Hoffmann (1990): Kinetics of Methyl Tertiary Butyl Ether liquid phase synthesis catalyzed by ion exchange resin – I. Intrinsic rate expression in liquid phase activities. Chem. Eng. Sci., 45 (6), 1605 – 1617.

18. M. Mazotti, B. Neri, D. Gelosa, A. Kruglov and M. Morbidelli (1997): Kinetics of liquid-phase esterification catalyzed by acidic resins. Ind. Eng. Chem. Res., 36, 3 – 10.

19. U. Weidlich and J. Gmehling (1987): A modified UNIFAC model. 1. Prediction of VLE, h^E and g^{∞}. Ind. Eng. Chem. Res., 26, 1372 – 1381.

20. P. Moritz, S. Blagov and H. Hasse (2001): Reactive distillation process design and scale-up. Proceedings Separations Technology Topical Conference, AIChE Annual Meeting 2001, Volume 2, ISBN0-8169-9762-4, 906-913.

21. A. Górak and A. Hoffmann (2001): Catalytic distillation in structured packings. AIChE Journal, 47 (5), 1067 – 1076.

KEYWORDS

- Reactive distillation experiments
- Hexyl acetate
- Catalytic packing
- Scale-up
- Modeling and simulation